

Upscaling Regional, 3D, Non-Fickian Solute Transport with 2D Equivalent Models

H43I-2582

AGU Fall Meeting 2018

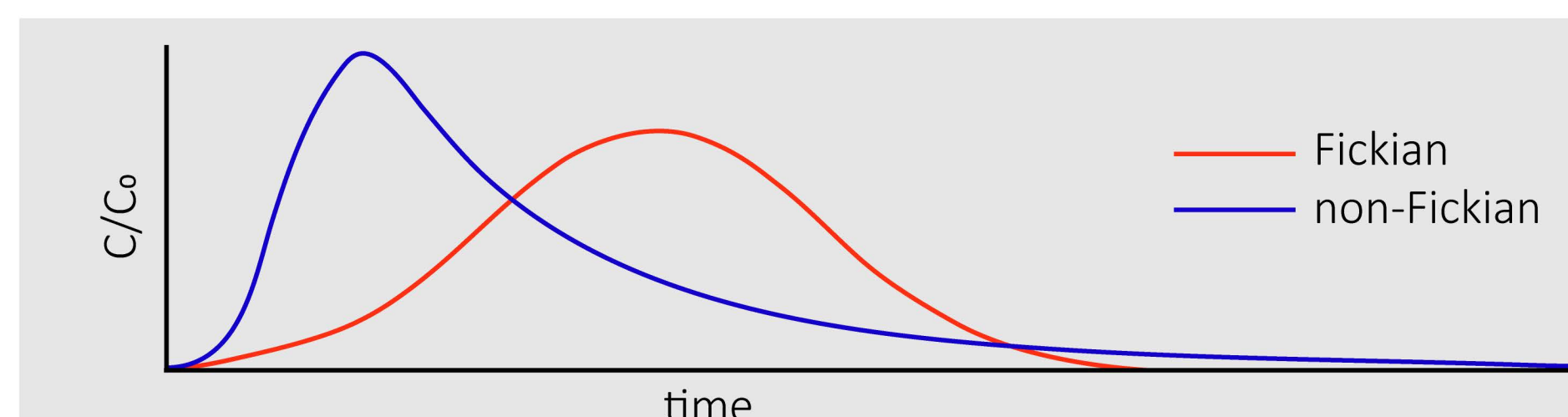
Washington, DC

Rich Pauloo^{1*} | Graham Fogg¹ | Zhilin Guo¹ | Christopher Henri¹
 [1] University of California, Davis | * corresponding author

1. BACKGROUND & MOTIVATION

CORE QUESTION:

Can non-Fickian contaminant transport effects produced by 3D heterogeneity be represented in 2D?



The past half century has witnessed the emergence of non-point source pollutants [1, 2] that challenge the sustainability of regional scale, fresh groundwater resources. For example, decreasing water quality associated with increases in Total Dissolved Solids (TDS) has been documented in aquifers across the United States in the past half century [3].

Conventional models of non-Fickian contaminant transport in porous media rely on detailed hydrogeologic characterization, in particular the representation of connected high-K pathways [4, 5, 6, 7], and a numerical solution of the advection dispersion equation (ADE).

These approaches work well at the field scale, but are computationally intractable at the basin scale. Thus, this research aims to develop simple, upscaled models of non-Fickian solute transport which are cheap to run at the regional scale, and easy to create.

The developed models will be used to evaluate closed basin salinization and other regional-scale, non-point source contamination issues.

2. APPROACH

1. Wessmann (1999) developed a 3D hydraulic conductivity domain from thousands of well logs and a transition probability geostatistical approach (T-PROGS) in the King's River Fan in California, USA [8]. Derive 63 2D realizations from this domain by taking "slices" along the zy plane. Let the set of all slices be called S , and individual slices, s_i . Then,

$$S = \{s_1, s_2, s_3, \dots, s_{63}\}$$

2. Solve the steady state groundwater flow problem by the finite difference method in MODFLOW for the 3D domain and all 2D slices.

3. Using the flow from 2., solve the ADE in the 3D domain and all 2D slices with the random walk particle tracking code RW3D [9]. For 3D domain and all 2D realizations, compare breakthrough curves (BTC), and Bianchi and Pedretti's (2006) transport connectivity indicator (TCI) [10].

4. If 2D transport can approximate 3D transport, use the developed T-PROGS model to simulate multiple 2D basin-scale realizations.

5. Using MODFLOW and RW3D, simulate:
 (a) business as usual groundwater quality evolution
 (b) climate change impacts to groundwater quality
 (c) effects of mitigative practices, e.g. managed aquifer recharge
 (d) water budget required to reverse closed basin salinization

3. CLOSED BASIN GROUNDWATER SALINIZATION

Legend:
 low TDS (light blue)
 medium TDS (orange)
 high TDS (red)
 groundwater well (grey circle)
 water budget terms (blue arrow)
 agriculture (green dots)

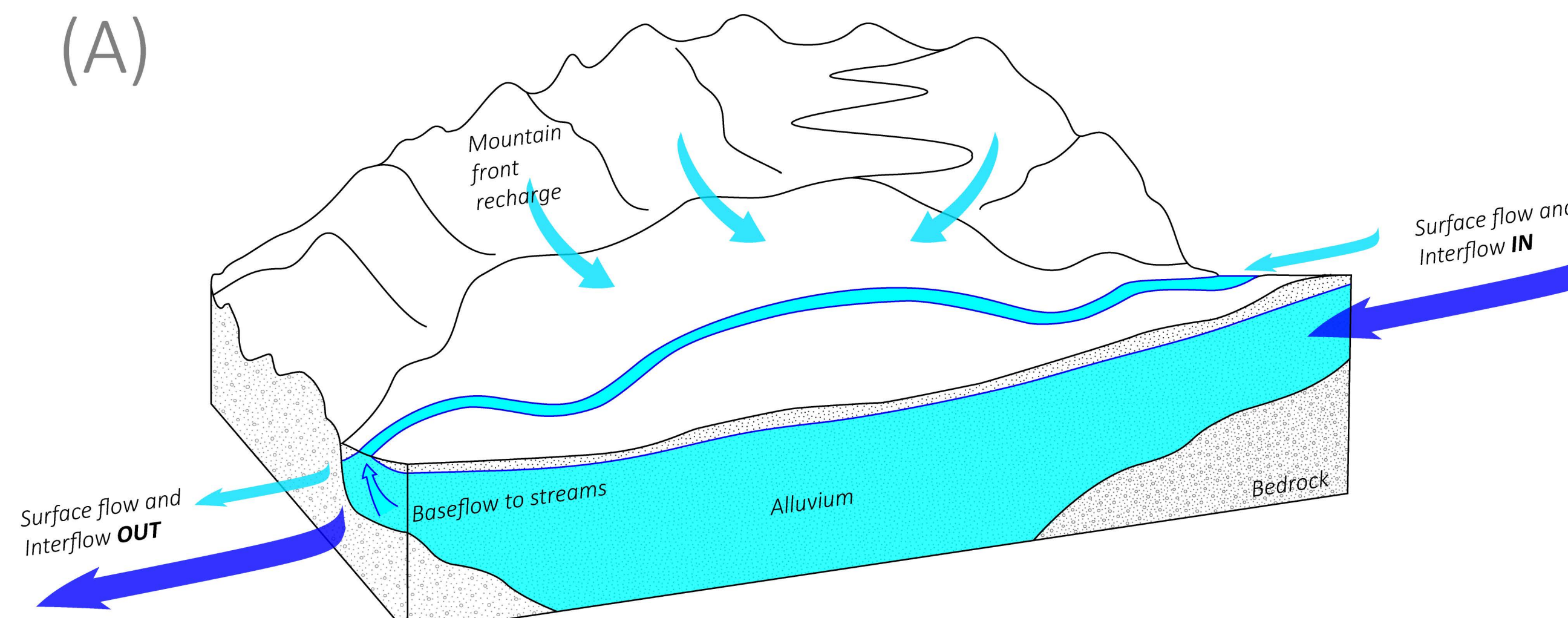


Figure 1A: Open basin, pre-groundwater development: surface and groundwater systems connect. Groundwater discharges dissolved solids into surface water which exit the basin. Groundwater at this stage is predominantly fresh (e.g., < 1,000 mg/L).

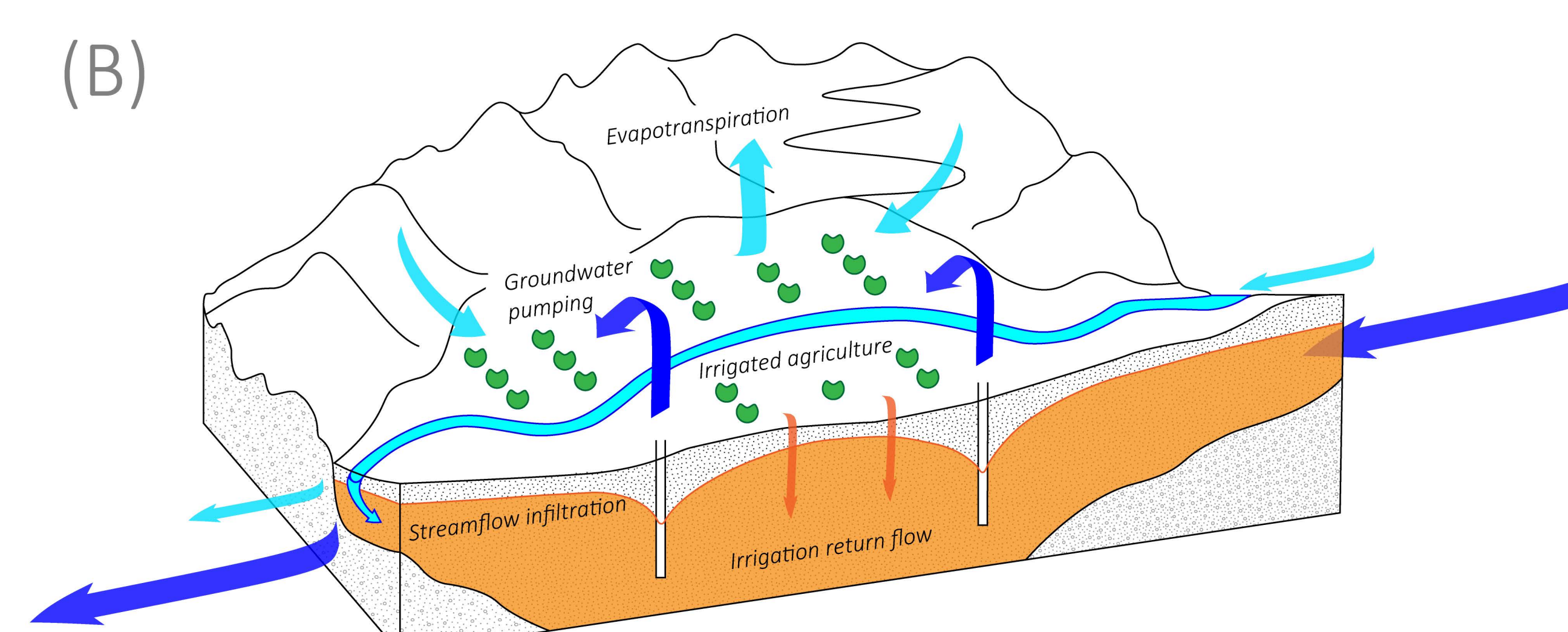


Figure 1B: Partial closure of basin: groundwater pumping causes reduction or elimination of baseflow to streams. Pumped groundwater returns to the basin via irrigation return flow. Dissolved solids begin to accumulate in groundwater.

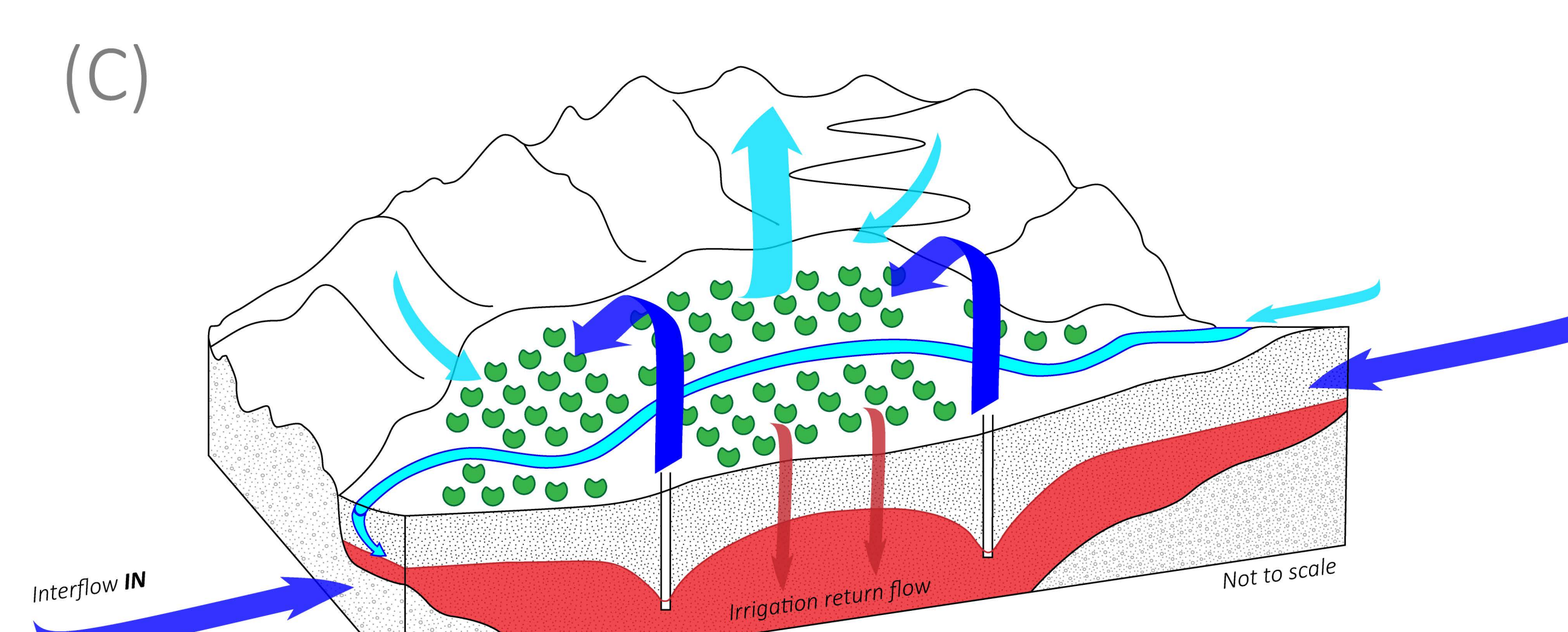


Figure 1C: Closed basin: falling groundwater levels cause subsurface interflow to drain adjacent basins. Streams lose to groundwater. Water primarily exits via evapotranspiration, which further concentrates dissolved solids in groundwater.

4. RESULTS

4.1 Geostatistical Transition Probability Model

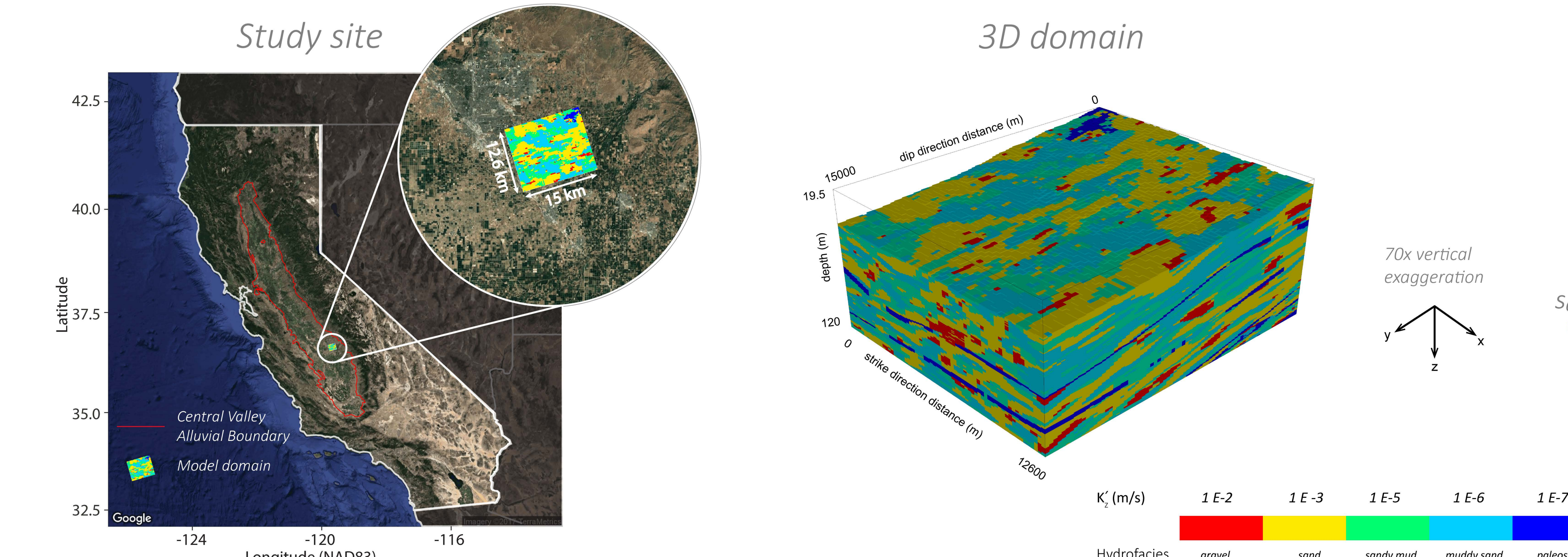


Figure 2: Study site in the Kings River Alluvial Fan, CA.

3D domain

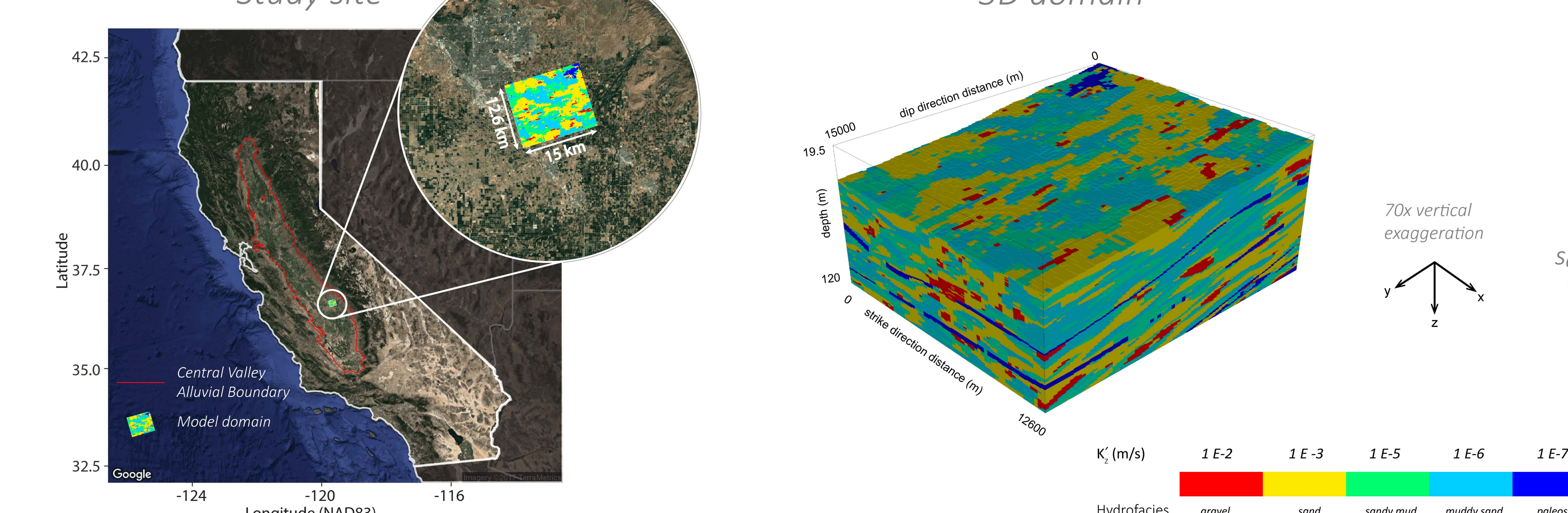


Figure 3: 3D transition probability model of 5 hydrofacies, with 3 representative 2D slices showcasing geologic features of the domain. Dimensions $(x,y,z) = (12.6\text{km}, 15\text{km}, 100.5\text{m})$. Discretization $(x,y,z) = (200\text{m}, 200\text{m}, 0.5\text{m})$. For more details see Weissmann et al. (1999) [8].

4.2 Steady State Flow Model

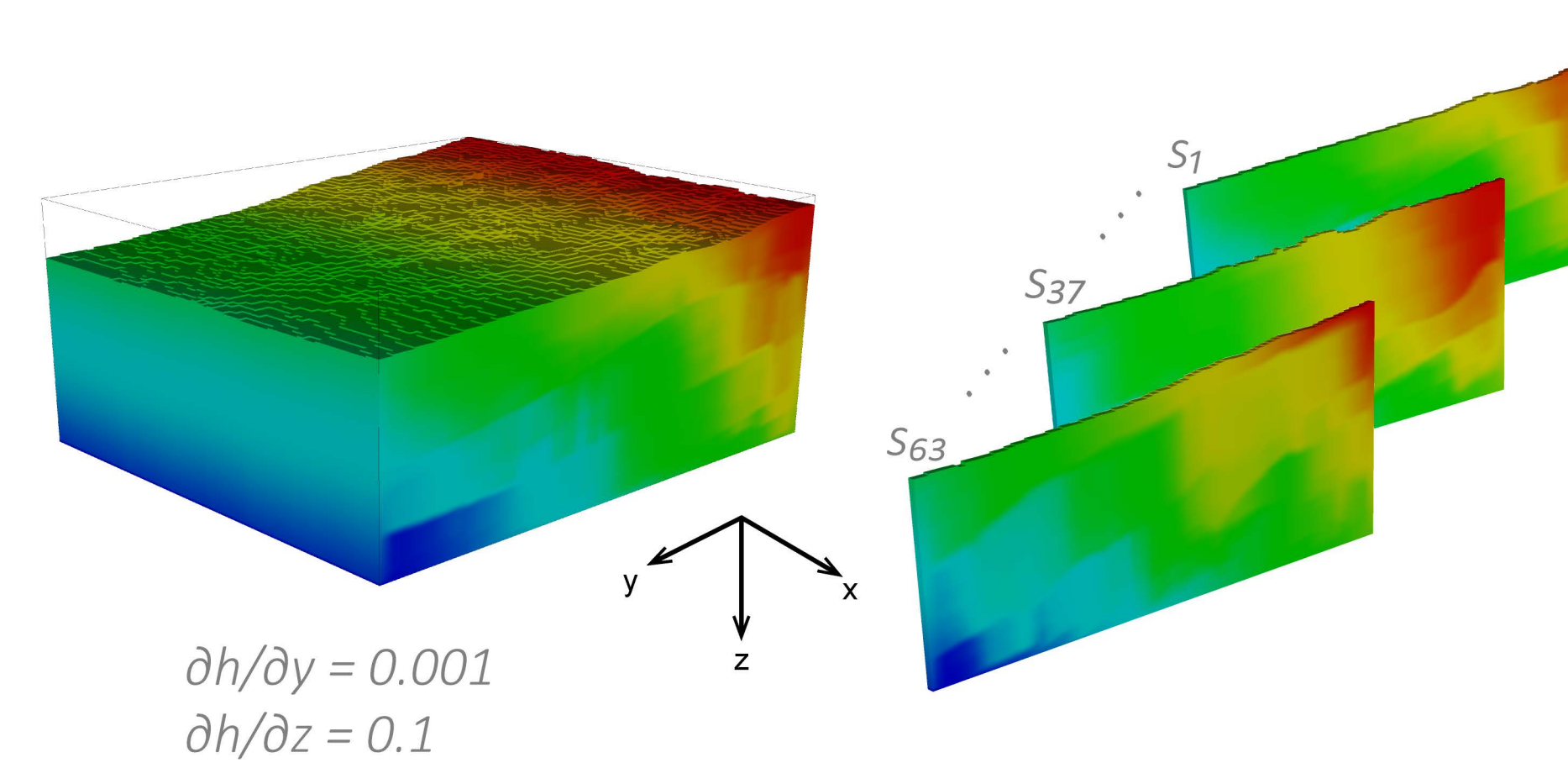


Figure 4: Head gradients for 3D domain and 3 representative 2D slices. Constant head boundary conditions across ZZ and YY faces. No flow across XX. $\frac{\partial h}{\partial z} = 100 \left(\frac{\partial h}{\partial y} \right)$, which is typical for this agriculturally intensive aquifer.

4.4 Transport Connectivity Indicators

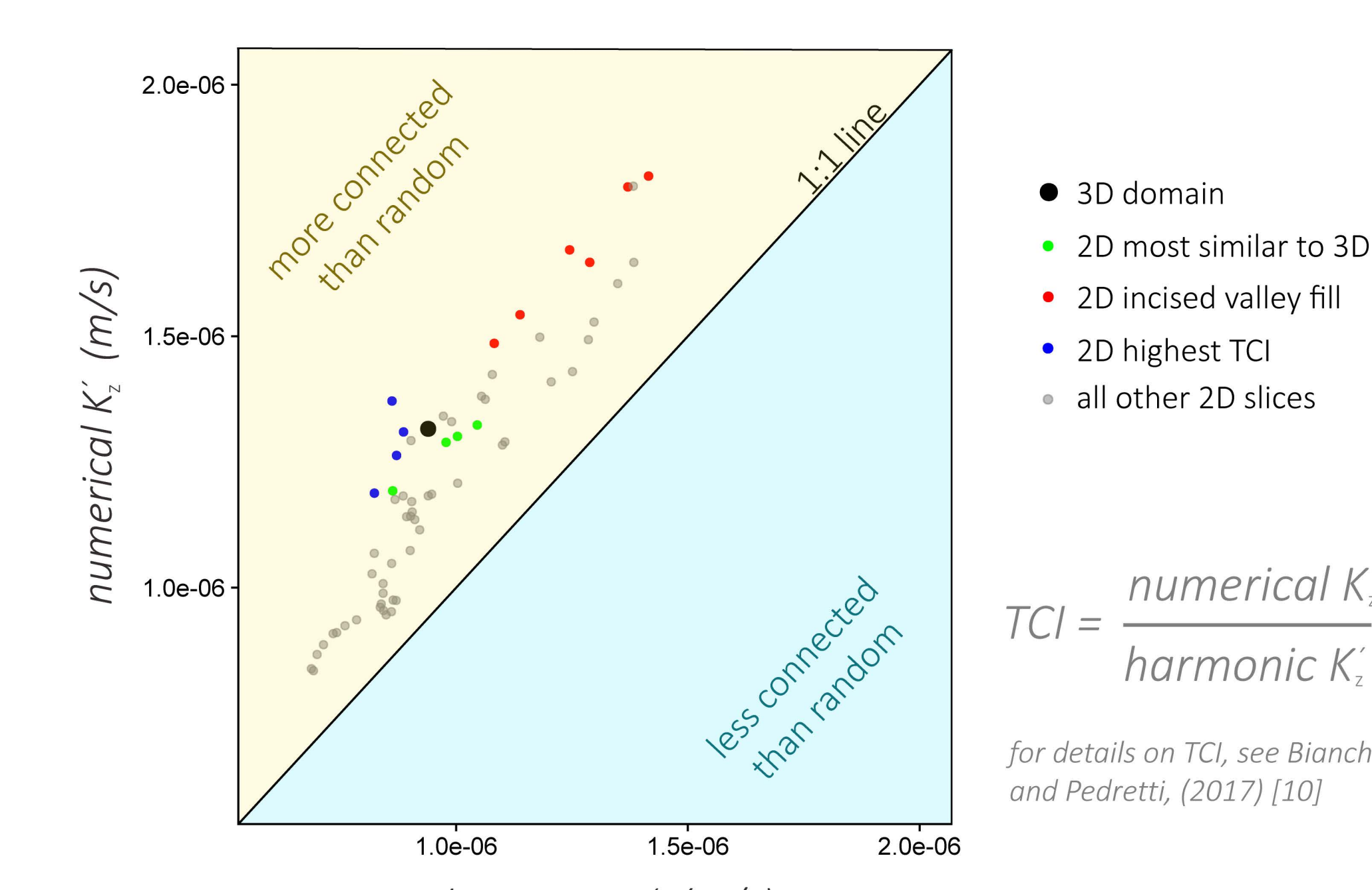


Figure 5: Breakthrough curves for 3D domain and all 2D slices. R-2D slices most similar to 3D domain. L-incised valley fill and high TCI slices. Non-point source pulse injection of 100,000 particles at 10m below land surface. Simulation time = 10,000 days (27.4 yrs). Standard Random Walk with Eulerian velocity integration. Dispersivity in $(x,y,z) = (2\text{m}, 2\text{m}, 0.05\text{m})$. No diffusion. No mass transfer.

5. DISCUSSION & FUTURE RESEARCH

The mean BTC of all 2D slices approximates the 3D BTC, thus an ensemble of 2D slices may provide a confidence interval for 3D transport. 2D slices require less particles to track, and are efficiently run in parallel, which may speed up simulations by ~100x.

Early arriving particles are explained by high-K and high-TCI facies, but the features of 2D slices that mimic 3D transport behavior are not yet explained. If these features are known, we need only run a few 2D slices to obtain 3D non-Fickian transport, and previously-intractable regional-scale problems will be solvable.

New Core Question: What are the features of 2D slices that make them good representatives of 3D BTCs?

Graph based approaches of representing geological networks like those described by Hyman et al. (2017) are a promising avenue to characterize 3D and 2D connected domains. 2D domains with similar graph efficiency to the 3D domain may exhibit similar BTCs.

6. ACKNOWLEDGEMENTS

This work was supported by NSF DGE # 1069333, the Climate Change, Water, and Society IGERT, to UC Davis, and by the U.S./China Clean Energy Research Center for Water-Energy Technologies (CERC-WET).



References

- [1] Buresh, J. C. (1986). Source Pollution Control Notes State and Federal Land Use Regulation: An Application to Groundwater and Nonpoint Source Pollution Control. *The Yale Law Journal*, 95(7), 1433–1458.
- [2] Nativ, R. (2004). The desert flowlines lessons learned from the Israeli case. *Ground Water*, 42(5), 651–657.
- [3] USGS. N. A. (2010). Water Quality in Principal Aquifers of the United States, 1991–2010 Circular 1360.
- [4] Fogg, G. E. (1986). Groundwater Flow and Sand Body Interconnectedness in a Thick, Multiple-Aquifer System. *Water Resources Research*, 22(5), 679–694. <https://doi.org/10.1029/WR022005p00679>
- [5] Webb, E. K., & Andersen, M. P. (1996). Simulation of preferential flow in three-dimensional, heterogeneous conductivity fields with realistic internal architecture. *Water Resources Research*, 32(3), 533–545. <https://doi.org/10.1029/WR939>
- [6] Fogg, G. E., & Labille, E. M. (2000). Connected Network Paradigm for the Alluvial Aquifer System.
- [7] Fogg, G. E., & Labille, E. M. (2009). Motivation of synthesis, with an example on groundwater quality sustainability. *Water Resources Research*, 45(9), L5–L5. <https://doi.org/10.1029/2008WR004372>
- [8] Weissmann, G. S., S. A. Carle, and G. E. Fogg. 1999. Three-dimensional hydrofacies modeling based on soil survey analysis and transition probability geostatistics. *Water Resources Research* 35 (6): 1761–70.
- [9] Fernandez-Garcia, D., Illangasekare, T. H., and Rajaram, H. (2005). Differences in the scale-dependence of dispersivity estimated from temporal and spatial moments in physically and chemically heterogeneous porous media. *Advances in Water Resources*, 28(9–10), 1309–1318.
- [10] Fogg, G. E., M. P. Pedretti, and G. E. Fogg. 2017. Geological network models for solute transport in heterogeneous porous media. *Water Resources Research*, 45(1), 4591–4702. <https://doi.org/10.1002/2016WR019095>
- [11] Hyman, J. D., Hagberg, A., Sriwisan, G., Mohd-Yusof, J., & Viswanathan, H. (2017). Predictions of first passage times in sparse discrete fracture networks using graph-based reductions. *Physical Review E*, 96(1), 1–10. <https://doi.org/10.1103/PhysRevE.96.013304>